Autonomous Characterization of Lithium-Ion Battery Model Parameters utilizing a Mathematical Optimization Methodology

Galo D. Astudillo, Hamzeh Beiranvand, Helge Krüger, Sandra Hansen, Marco Liserre
Chair of Power Electronics, KIEL UNIVERSITY
Kaiserstraße 2, 24143 Kiel
Kiel, Germany
Phone: +49 431 880-6100
Fax: +49 431 880-6103
Email: danielastudilloheras@gmail.com,{hab,hkr,sn,ml}@tf.uni-kiel.de
URL: http://www.pe.tf.uni-kiel.de

Christian Werlig, Andreas Würsig
Fraunhoffer ISIT
Fraunhoferstraße 1
Itzehoe, Germany
Phone: +49 4821 17-0
Fax: +49 4821 17-4250
{christian.werlich,andreas.wuersig}@isit.fraunhofer.de
URL: https://www.isit.fraunhofer.de/

Acknowledgment

Funded by the European Union - European Regional Development Fund (EFRE), the German Federal Government and the State of Schleswig-Holstein (LPW-E/1.1.2/1486).

Keywords

≪State of Charge≫, ≪Optimization≫, ≪Batteries≫, ≪Electric Vehicle≫.

Abstract

Kalman filtering is commonly used for state-of-charge (SOC) estimation for lithium-ion (Li-ion) batteries owing to its simplicity, computational efficiency, and relatively precise results. However, kalman filters depend on the Li-ion battery model. Several laboratory tests such as incremental current and dynamic stress tests are required to determine battery model parameters in model-based SOC estimation. These tests such as incremental current test and dynamic stress test are time-consuming and can take multiple days. A mathematical optimization along with a battery test method, which does not need rest time for battery, are adopted to reduce the battery parameter identification time, drastically. A mathematical optimization stage is embedded prior to Kalman Filter based SOC estimation computing the battery open circuit voltage (OCV) and as well as an initial guess of the RC parameters of the battery equivalent circuit. Therefore, it reduces the required number of tests to one. Extensive numerical studies on a 2 Ah Lithium-ion cell verify the effectiveness of the proposed method by achieving a RMS error less than one percent.

I. Introduction

The battery management system (BMS) controls the charging/discharging process and guarantees the safety by permanent monitoring and parameter estimation of the electric vehicles (EVs) battery packs [1].

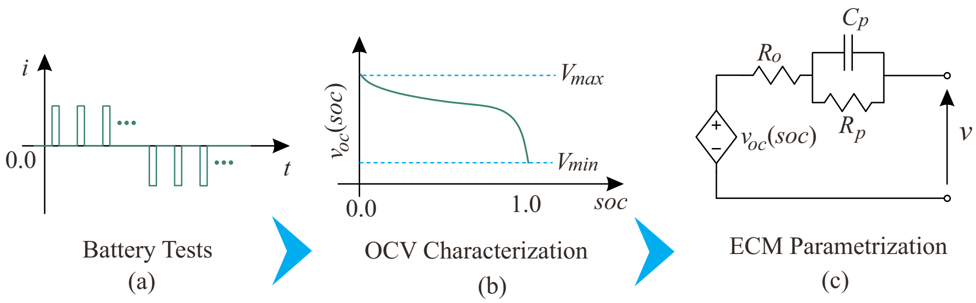

Fig. 1: Conventional process for ECM parameter characterization for lithium-ion batteries v_{oc}: (a) battery test current profile, (b) OCV voltage characterization, and (c) model parameter estimation.

An accurate estimation of the battery state-of-charge (SOC) is a prerequisite to achieve the expected functions of the BMS.

Battery SOC estimation techniques have received a significant attention in both academia and industry due to its central role in the BMS. These methodologies can be classified into coulomb counting, lookup table, data-driven approaches, model-based approaches, and hybrid methods [2]. Surveys in [3, 4] show that model-based methods are the most promising solutions and are widely used in EV applications. Among the model-based approaches, equivalent circuit model (ECM) is preferred over electrochemical models (e.g. single particle model [5]) for SOC estimation owing to its computational efficiency, direct connection to coulomb counting and simple implementation of the Kalman filter family observers as the state-of-the-art solution [6]. However, efficient exploitation of the ECM model is subject to precisely estimate and calibrate the ECM parameters including open circuit voltage (OCV), RC pairs and the equivalent internal resistance.

The characterization of the variable voltage source is usually performed with an OCV test that provides pairwise values of the terminal voltage of the battery after a long relaxation time and the corresponding SOC [7]. To obtain the OCV-SOC curve, laboratory tests such as incremental current (IC) tests, low current (LC) tests at a very small C-rate (e.g. $\frac{1}{20C}$) or combined tests (CT) are required [8]. In the case of the IC tests, long relaxation times are needed to reach the near equilibrium potential. On the other hand, LC tests discharge/charge the battery at a small C-rate consuming a significant time. In addition to IC tests, a second dynamic current test is usually required to obtain the remaining parameters of the ECM. Nonetheless, these tests are time consuming and as a result autonomous characterization methods, independent from test types, are required.

The motivation behind this work is to tackle with the problem of the lithium-ion battery ECM parameterization not only for fresh cells with minimum test requirements but also to calibrate the model parameters during the operation and compensate for the SOC estimator degradation due to cell aging and sensor drifting.

A two-stage optimization process is proposed to increase the SOC estimation performance. In the fist stage, the OCV-SOC characterization is formulated as an optimization problem and solved by newton-based optimization approaches in a long time horizon. The time horizon could be tens of cycle or few months depending on the application. The second stage is to find the ECM parameters in the sample horizon to contribute to the unscented Kalman filter (UKF) based SOC estimation by providing a relatively precise initial guess of the ECM parameters. An advantage of using the UKF instead of the Extended Kalman Filter (EKF) is that the first one achieves at least 2nd order accuracy, while the EKF provides 1st order accuracy on the propagation of the state distribution [9]. Extensive numerical studies are carried out on lithium-ion batteries and the results are compared with the existing literature. The obtained results verify the effectiveness of the proposed mathematical optimization based approach for ECM characterization and SOC parameter estimation of the lithium-ion batteries. It is shown that ECM can be equaly parameterized by different tests such as IC test, Federal Urban Driving Schedule (FUDS), Highway Driving Schedule (US06) and Beijing Dynamic Stress Test (BJDST), and the Dynamic Stress Test (DST) utlizing the proposed autonomous characterization technique.

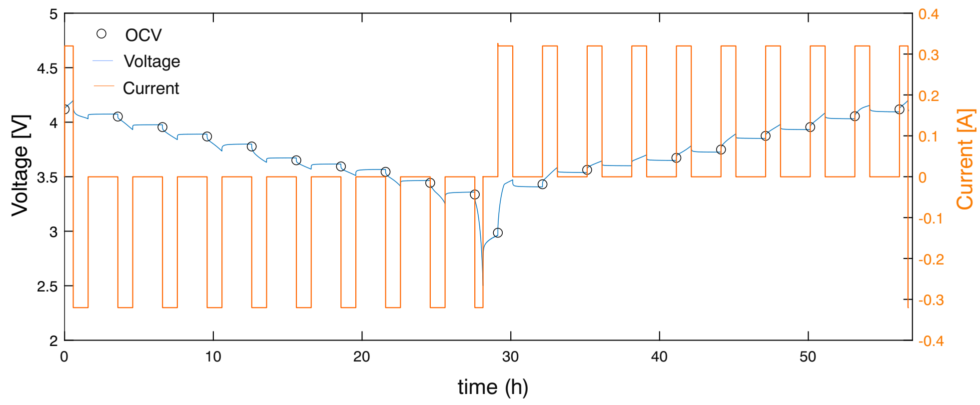

Fig. 2: A typical IC test for characterizing OCV.

II. Battery Modeling

The simplified model of the battery cell using an equivalent electric circuit is presented in Fig 1 as well as the conventional process of ECM characterization. This representation greatly reduces the complexity of the modeling of the battery by characterizing it with a RC circuit. The first order ECM is characterized with following equations:

$$\frac{d}{dt}v_c(t) = -\frac{v_c(t)}{R_pC_p} + \frac{i(t)}{C_p} \quad (1)$$

$$v(t) = i(t)R_o + v_c(t) + v_{oc}(soc(i(t))) \quad (2)$$

$$soc(i(t)) = soc_o + \frac{\eta}{C_{bat}} \int i(t)dt \quad (3)$$

where the capacitor voltage is $v_c(t)$, the terminal voltage is $v(t)$, the state of charge is soc. The capacity of the battery is denoted by C_{bat}. In addition, v_{oc} is the open-circuit voltage, i is the current and η is the coulomb efficiency. R_o, R_p, and C_p are the ECM parameters.

Results of [10] show that it is not necessary to perform a temperature-dependent OCV-SOC characterization if the battery capacity is "estimated dynamically and continuously". Therefore, the dependancy of OCV-SOC on temperature is neglected. Furthermore, we assume R_o, R_p and C_p to be fixed during the parametrization of the ECM at a given temperature T, which could be the nominal temperature.

III. OCV-SOC characterization

A set of experiments are carried out to show the typical IC test requirements for OCV-SOC characterization. An IC test at a current rate of C/10 with relaxation times of 2 hour is conducted on a 1865 cell with 3200 mAh capacity from LG employing a battery cycler (Biologic, VSP3e) and the results are shown in Fig. 2. Normally, OCV is defined as the equilibrium potential after setting the current to zero for a long time as can be seen from the experimental results. Theoretically, OCV can be achieved at minimum Gibbs free energy resulting from the overall electrochemical reactions in the battery cell [11]. Since the parasitic processes such as corrosion continue, OCV is interpreted as the first plateau after the relaxation of the most relevant reactions in the cell [12]. However, these kinds of tests which are associated with battery relaxation require a lot of time as demonstrated in Fig. 2. Thereby, other test methods as in [13] shall be considered in battery model calibration and characterization.

In the literature, OCV-SOC curves have been represented with look-up tables or many analytical functions (e.g. sigmoid, polynomial, exponential, chebyshev, logaritmic, etc). The OCV-SOC curve fitting procedure comparing several suitable functions can be found in [10]. In general, fitting the curve with a polynomial is one the most accurate and simplest approaches [8, 10, 14–16]. Hence, due to its simplicity and accuracy, we consider a polynomial function of the following form:

$$v_{oc}(soc) = \sum_{l=0}^{n} a_l soc^l \tag{4}$$

where n is the degree of the polynomial and a_l ($\forall l \in \{0,1,...,n\}$) are the coefficients. Now, it is important to notice the characteristics of $v_{oc}(soc)$ to establish a proper formulation of the fitting problem in hand. The main characteristics that will be included in the formulation are:

1. The maximum (V_{max}) and minimum (V_{min}) value of the terminal voltage at the equilibrium potential are known (i.e. when $soc = 1$ and $soc = 0$). Such parameters are usually known beforehand, and they establish the boundaries of $v_{oc}(soc)$ as $v_{oc}(0) = V_{min}$ and $v_{oc}(1) = V_{max}$.

2. The function $v_{oc}(soc)$ is monotonically increasing $\forall\ soc\ \in [0,1]$.

3. The curvature of the $v_{oc}(soc)$ is non-positive when $soc = 0$ (e.g. $\frac{d^2}{d\,soc^2} v_{oc}(soc)|_{soc=0} \leq 0$) and non-negative when $soc = 1$ (e.g. $\frac{d^2}{d\,soc^2} v_{oc}(soc)|_{soc=1} \geq 0$).

4. Due to the polarization, depending on the sign of the current $v_{oc}(soc)$ can be greater or smaller than the terminal voltage. If the current is negative (discharging) then $v_k < v_{oc}(soc_k)$ and if the current is positive (charging) $v_k > v_{oc}(soc_k)$.

The considerations presented above need to be included in the optimization problem. To do that, we first consider N samples, and separate each $k-th$ sample for $K = \{K^+ \cup K^0 \cup K^-\}$ where $K^+ = \{k \in \mathbb{Z}^+ : i_k > 0\}$, $K^o = \{k \in \mathbb{Z}^+ : i_k = 0\}$, and $K^- = \{k \in \mathbb{Z}^+ : i_k < 0\}$. The unknown variables are included in the vector $c = [a_0, a_1, \cdots, a_n]^T$. Finally, the constrained optimization problem is defined as follows:

$$\underset{c}{\text{argmin}} := f^+(c) + f^-(c) + f^o(c) \tag{5}$$

where

$$f^+(c) := \sum_{k \in K^+} \frac{1}{2} max(0, v_{oc}(soc_k) - v_k)^2 \tag{6}$$

$$f^-(c) := \sum_{k \in K^-} \frac{1}{2} max(0, v_k - v_{oc}(soc_k))^2 \tag{7}$$

$$f^o(c) := \sum_{k \in K^o} \frac{1}{2} (v_{oc}(soc_k) - v_k^*)^2 \tag{8}$$

constrained to equality and inequality constraints as:

$$\begin{aligned} h_1 &:= \sqrt{N}(v_{oc}(1) - V_{max}) = 0 \\ h_2 &:= \sqrt{N}(v_{oc}(0) - V_{min}) = 0 \end{aligned} \tag{9}$$

$$\begin{aligned} g_1 &:= -\sqrt{N}\left(\frac{d^2}{d\,soc^2} v_{oc}(soc)\Big|_{soc=1}\right) \leq 0 \\ g_2 &:= \sqrt{N}\left(\frac{d^2}{d\,soc^2} v_{oc}(soc)\Big|_{soc=0}\right) \leq 0 \end{aligned} \tag{10}$$

Note that the formulation of Eq. (5) is based on the penalty method. Hence, a third cost $f^0(c)$ is included in order to keep $v_{oc}(soc_k)$ in the neighborhood of v_k when $i_k = 0$. For the optimization problem, the experimental test (i.e. the current profile) is expect to have as much variation as possible. Therefore, both discharge and charge currents should be part of such test, as well as some zero currents where relaxation time is not necessarily required. An example of a profile that contains the aforesaid variations is the FUDS profile. The constraints are scaled by a factor of $\sqrt{N}$ to include a proper weight considering the number of data points available.

IV. Parameter Estimation

IV.a ECM parametrization

After that v_{oc} is determined, the second step is to obtain optimal values for $\boldsymbol{p} = [R_o, R_p, C_p]^T$. For this task, a formulation in the discrete-time domain for the future terminal voltage v_{k+1} is developed. Hence, Eq. (1) is solved for a small step $\delta = \Delta T$ and a current $i[k]$ during the k-th interval:

$$v_{ck+1} = v_{ck} e^{-\delta/C_p R_p} + i_k R_p (1 - e^{-\delta/R_p C_p}) \tag{11}$$

Next, a discrete version of Eq. (3) is obtained with the bilinear transformation:

$$soc_{k+1} = soc_k + \frac{\delta}{2C_{bat}} (i_k + i_{k-1}) \tag{12}$$

Moreover, the terminal voltage can be represented as:

$$v_k = i_k R_o + v_{ck} + v_{oc}(soc_k) \tag{13}$$

$$v_{k+1} = i_{k+1} R_o + v_{ck+1} + v_{oc}(soc_{k+1}) \tag{14}$$

Substituting Eq. (11) in Eq. (14) results in:

$$v_{k+1} = i_{k+1} R_o + v_{ck} e^{-\delta/C_p R_p} + i_k R_p (1 - e^{-\delta/R_p C_p}) + v_{oc}(soc_{k+1}) \tag{15}$$

Finally, solving for v_{ck} from Eq. (13) and replacing it in Eq. (15):

$$\begin{aligned} v_{k+1} = {} & i_{k+1} R_o + (v_k - i_k R_o - v_{oc}(soc_k)) e^{-\delta/C_p R_p} + i_k R_p (1 - e^{-\delta/R_p C_p}) \\ & + v_{oc}(soc_{k+1}) \end{aligned} \tag{16}$$

Note that R_o, R_p, C_p are the only unknowns, since soc_{k+1} is obtained with Coulomb counting with Eq. (12). To find these unknown variables, the problem is formulated as the following optimization problem:

$$\underset{\boldsymbol{p}}{\operatorname{argmin}} := \sum_{k=1}^{N} \frac{1}{2} (v_{k+1}(p) - v^*_{k+1})^2 \tag{17}$$

where v^*_{k+1} is the future sample of the terminal voltage. It is important to mention that in this formulation there is not separating the sample points, since the N available data points are used in this task. Hence, such problem is relatively easy to solve with unconstrained optimization techniques. The proposed objective functions are solved using Sequential Least Squares Programming (SLSQP).

IV.b SOC estimation with UKF

After obtaining optimal values for the coefficients of the OCV-SOC curve and the ECM, we aim use this values in the model for the SOC estimation and terminal voltage prediction. For this task, an UKF is adopted. The UKF utilizes a discretized version of the nonlinear dynamic system of the following form:

$$\boldsymbol{x_{k+1}} = f(\boldsymbol{x_k}, i_k) + \boldsymbol{w_k}, \; y_k = g(\boldsymbol{x_k}) + u_k \tag{18}$$

Where x_k is the vector of states, w_k and v_k are the process and the observation noise, respectively. The function f is a mapping between the prediction of the future state $\boldsymbol{x}_{k+1}$ given the current state $\boldsymbol{x_k}$, while the function g returns the observation. The state distribution is represented by a Gaussian random variable, and it is specified by sample points that capture the statistics (e.g. mean and covariance) of the state distribution. Moreover, the propagation of this statistics through the system (i.e. $f(\boldsymbol{x_k}, i_k) + \boldsymbol{w_k}$) captures the posteriori mean and covariance with the unscented transformation (UT). Now, the space state representation of the ECM can be formulated as follows:

$$\boldsymbol{x_{k+1}} = \boldsymbol{A_k x_k} + i_k \boldsymbol{B_k} + \boldsymbol{w_k} \tag{19}$$

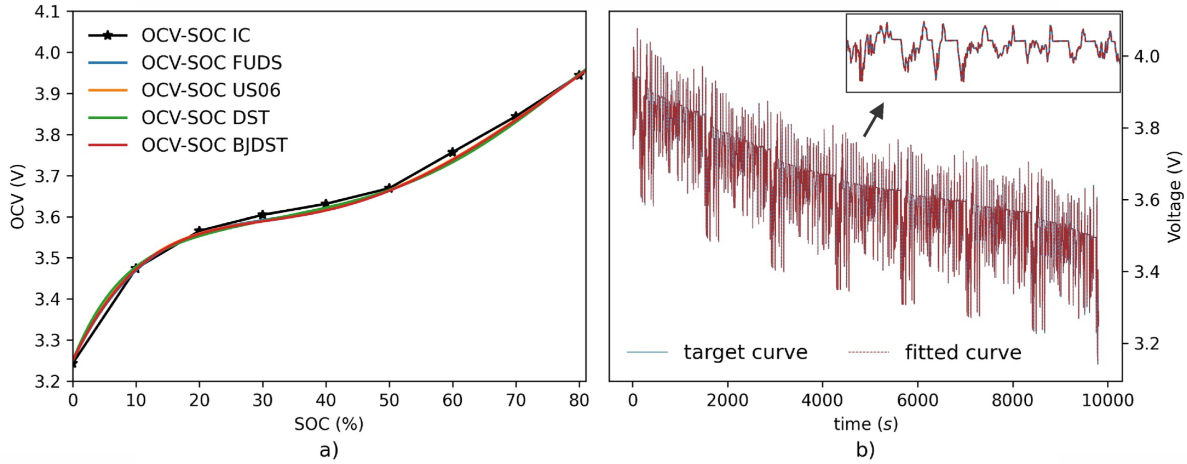

Fig. 3: a) OCV-SOC curves comparing incremental current test vs data-driven characterization at 25 ^{o}C and b) Curve-fitting ECM with data from FUDS.

with the following measurement equation:

$$y_k = i_k R_{ok} + v_{ck} + v_{oc}(soc_k) + u_k \tag{20}$$

with

$$\boldsymbol{x_k} = \begin{bmatrix} soc_k \\ v_{ck} \\ R_{ok} \end{bmatrix}, \boldsymbol{A_k} = \begin{bmatrix} 1 & 0 & 0 \\ 0 & e^{-\delta/\tau} & 0 \\ 0 & 0 & 1 \end{bmatrix}, \boldsymbol{B_k} = \begin{bmatrix} \delta/C_{bat} \\ R_p(1-e^{-\delta/\tau}) \\ 0 \end{bmatrix}, \boldsymbol{w_k} = \begin{bmatrix} w_{soc k} \\ w_{v_c k} \\ w_{R_o k} \end{bmatrix} \tag{21}$$

where C_{bat} is the capacity of the battery, δ is the sampling time, and τ is the time constant ($\tau = R_p C_p$). The function v_{oc} returns the OCV of the circuit given the SOC. In addition, the vector $\boldsymbol{w_k}$ and the scalar u_k are zero-mean Gaussian stochastic processes with a known covariance $\boldsymbol{Q}_{w_k}$ and R_{u_k}, respectively.

V. Numerical Studies

To carry out a comparative study, experimental data of a LiNiMnCo-cathode Graphite-anode battery from [17] are used. This data set has been used as a benchmark in some researches [18, 19]. However, the current intention is to obtain the OCV-SOC curves at 25ºC from four current stress tests, with three of them derived from driving cycles: Federal Urban Driving Schedule (FUDS), Highway Driving Schedule (US06) and Beijing Dynamic Stress Test (BJDST), and the Dynamic Stress Test (DST). The OCV-SOC characterization, ECM parametrization and UKF-based SOC estimation are explained in the followings:

OCV-SOC characterization: To evaluate the robustness, the proposed optimization method for OCV-SOC characterization is applied to all the test data (e.g. FUDS, US06, BJDST, and DST) and the results compared versus IC test as the reference value (v_{oc}^{*}). The obtained OCV-SOC curves are shown in Fig. 3 (a). This calibration process can be performed after few cycles autonomously without disconnecting the EV from the operation.

ECM parametrization: The second step is to utilize the obtained OCV-SOC curve for estimating temporary ECM parameters before applying UKF. Considering that FUDS could reflect the expected power variations in EV applications, it was selected to obtain the parameters of the ECM. This profile has been selected because of its complexity and it distribution of discharge/charge/zero currents: 55 %, 25 %, 20 %; respectively. The obtained parameters are Listed in Table I and compared versus the results of [19].There is a very small variation in the optimal values of the ECM parameters. The internal battery resistances R_o are very similar. Nonetheless, the parameters of the RC branch have noticeable differences. Fig. 3 (b) demonstrates the quality of the fitted terminal voltage achieved from the proposed methodology despite the considerable differences in RC paper with [19].

UKF-based SOC estimation: Once the FUDS profile has been utilized for finding the values of the

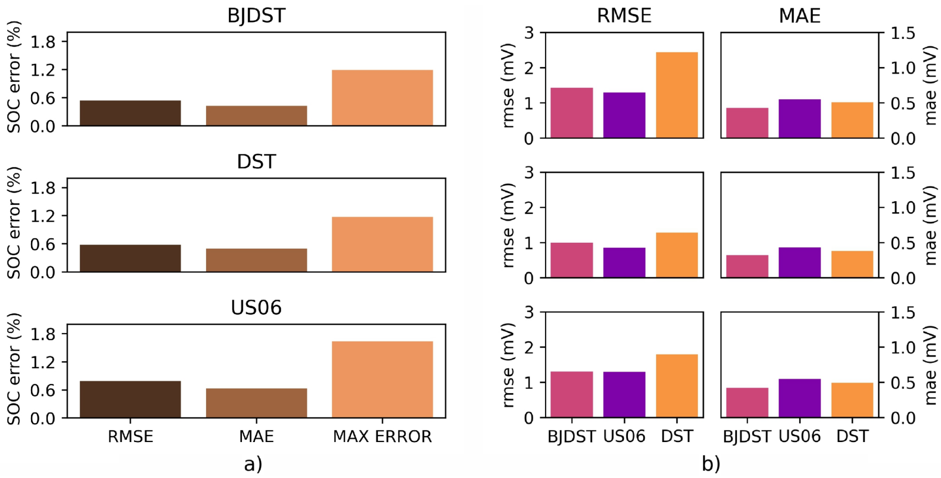

Fig. 4: Estimation and prediction errors: a) SOC at nominal SOC_o and b) Terminal voltage: First row considers $-10\,\%SOC_o$ error, second row SOC_o, and third row $+10\,\%SOC_o$.

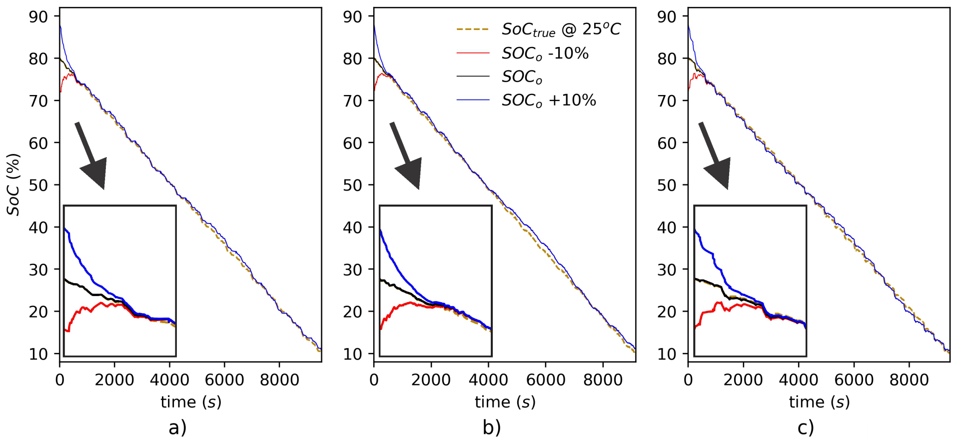

Fig. 5: SOC estimation considering an initial error using the same parameters obtained from FUDS and tested on: a) BJDST b) US06 and c) DST .

OCV-SOC and the ECM, the other three tests (BJDST, US06, DST) are adopted to validate the model. This procedure is carried out with the data from each test. Moreover, an error in the initial SOC is added (±10%) to monitor the response of the observer (i.e. UKF). The values of the covariance for the implementation of the UKF are selected as $R_{u_k} = 1e-6$ and $Q_{w_k} = diag([1e-6, 1e-4, 1e-4])$. Fig. 4 shows a summary of the RMSE and MAE of the SOC estimation and terminal voltage prediction on each test, varying the initial SOC and considering percentage values (i.e. 0%<SOC<100%). Moreover, these results are close to the results presented in [19], except for the maximum error. The maximum errors of US06 and and BJDST presented in Fig 4 a) are both ~ 50 % smaller in the proposed methodology.

The SOC estimation with each stress test and the introduced ±10% are also shown in Fig. 5. The results show that in despite of the introduced error of ±10% in the initial SOC, the estimator successfully corrects the wrong initial SOC.

Table I: The optimized ECM parameters with FUDS data in comparison with IC test + DST in [19]

	Parameters	Proposed Methodology	Reference [19]
ECM Parameters	R_o (Ω)	0.07152	0.0710
	R_p (Ω)	0.01544	0.0342
	C_p (F)	881.99	1135.2
Curve-fitting Error	MAE (V)	5.424e-4	3.708e-4
	$RMSE$	8.905e-4	5.988e-4

VI. Conclusions

The conventional open circuit voltage versus state-of-charge (OCV-SOC) characterizations based on incremental current test (ICT) and dynamic stress test (DST) are time consuming and a complete process could take several weeks in laboratory environment. Moreover, the re-calibration of battery OCV-SOC after a specific number of cycles is required to compensate the cell degradation effects on the OCV-SOC curve. Therefore, autonomous and robust OCV-SOC characterization respective to the battery test method becomes an inevitable task in applications such as electric vehicles. This paper presents a methodology for autonomous equivalent circuit model (ECM) parameter characterization without the need for time-consuming ICT and DST. Characterization process is formulated as an optimization problem and integrated prior to the unscented kalman filter based SOC estimation. The methodology can be implemented in real-time in low-cost micro-controllers as the problem is solved by newton-based mathematical methods. Numerical studies are carried out to validate the effectiveness of the proposed method. In the worst case scenario the SOC estimation root mean square error (RMSE) is confined to 1% and maximum error to less than 2% when there is an error of $\pm 10\%$ in the initial SOC. Therefore, the methodology is robust and able to autonomously characterize the OCV-SOC curves and estimate the ECM parameters in real-time.

References

[1] H. Rahimi-Eichi, U. Ojha, F. Baronti, and M.-Y. Chow, "Battery Management System: An Overview of Its Application in the Smart Grid and Electric Vehicles," *IEEE Industrial Electronics Magazine*, vol. 7, no. 2, pp. 4–16, Jun. 2013.

[2] D. N. How, M. Hannan, M. H. Lipu, and P. J. Ker, "State of charge estimation for lithium-ion batteries using model-based and data-driven methods: A review," *Ieee Access*, vol. 7, pp. 136 116–136 136, 2019.

[3] Y. Zheng, M. Ouyang, X. Han, L. Lu, and J. Li, "Investigating the error sources of the online state of charge estimation methods for lithium-ion batteries in electric vehicles," *Journal of Power Sources*, vol. 377, pp. 161–188, 2018.

[4] J. Meng, M. Ricco, G. Luo, M. Swierczynski, D.-I. Stroe, A.-I. Stroe, and R. Teodorescu, "An overview and comparison of online implementable soc estimation methods for lithium-ion battery," *IEEE Transactions on Industry Applications*, vol. 54, no. 2, pp. 1583–1591, 2017.

[5] W. Li, Y. Fan, F. Ringbeck, D. Jöst, X. Han, M. Ouyang, and D. U. Sauer, "Electrochemical model-based state estimation for lithium-ion batteries with adaptive unscented kalman filter," *Journal of Power Sources*, vol. 476, p. 228534, 2020.

[6] X. Bian, Z. Wei, J. He, F. Yan, and L. Liu, "A two-step parameter optimization method for low-order model-based state-of-charge estimation," *IEEE Transactions on Transportation Electrification*, vol. 7, no. 2, pp. 399–409, 2020.

[7] I. Snihir, W. Rey, E. Verbitskiy, A. Belfadhel-Ayeb, and P. H. Notten, "Battery open-circuit voltage estimation by a method of statistical analysis," *Journal of Power Sources*, vol. 159, no. 2, pp. 1484–1487, 2006.

[8] Y. Li, H. Guo, F. Qi, Z. Guo, and M. Li, "Comparative study of the influence of open circuit voltage tests on state of charge online estimation for lithium-ion batteries," *IEEE Access*, vol. 8, pp. 17 535–17 547, 2020.

[9] E. Wan and R. Van Der Merwe, "The unscented Kalman filter for nonlinear estimation," in *Proceedings of the IEEE 2000 Adaptive Systems for Signal Processing, Communications, and Control Symposium (Cat. No.00EX373)*. Lake Louise, Alta., Canada: IEEE, 2000, pp. 153–158.

[10] B. Pattipati, B. Balasingam, G. Avvari, K. Pattipati, and Y. Bar-Shalom, "Open circuit voltage characterization of lithium-ion batteries," *Journal of Power Sources*, vol. 269, pp. 317–333, Dec. 2014.

[11] P. Vágner, R. Kodỳm, and K. Bouzek, "Thermodynamic analysis of high temperature steam and carbon dioxide systems in solid oxide cells," *Sustainable Energy & Fuels*, vol. 3, no. 8, pp. 2076–2086, 2019.

[12] D. del Olmo, M. Pavelka, and J. Kosek, "Open-circuit voltage comes from non-equilibrium thermodynamics," *Journal of Non-Equilibrium Thermodynamics*, vol. 46, no. 1, pp. 91–108, 2021.

[13] T. Mamo and F.-K. Wang, "Long short-term memory with attention mechanism for state of charge estimation of lithium-ion batteries," *IEEE Access*, vol. 8, pp. 94 140–94 151, 2020.

[14] X. Hu, S. Li, H. Peng, and F. Sun, "Robustness analysis of State-of-Charge estimation methods for two types of Li-ion batteries," *Journal of Power Sources*, vol. 217, pp. 209–219, Nov. 2012.

[15] C. Weng, J. Sun, and H. Peng, "An Open-Circuit-Voltage Model of Lithium-Ion Batteries for Effective Incremental Capacity Analysis," in *Volume 1*. Palo Alto, California, USA: American Society of Mechanical Engineers, Oct. 2013, p. V001T05A002.

[16] Q.-Q. Yu, R. Xiong, L.-Y. Wang, and C. Lin, "A Comparative Study on Open Circuit Voltage Models for Lithium-ion Batteries," *Chinese Journal of Mechanical Engineering*, vol. 31, no. 1, p. 65, Dec. 2018.

[17] "Battery Research Overview | Center for Advanced Life Cycle Engineering." [Online]. Available: https://calce.umd.edu/battery-research-overview

[18] Y. Xing, W. He, M. Pecht, and K. L. Tsui, "State of charge estimation of lithium-ion batteries using the open-circuit voltage at various ambient temperatures," *Applied Energy*, vol. 113, pp. 106–115, Jan. 2014.

[19] F. Zheng, Y. Xing, J. Jiang, B. Sun, J. Kim, and M. Pecht, "Influence of different open circuit voltage tests on state of charge online estimation for lithium-ion batteries," *Applied Energy*, vol. 183, pp. 513–525, Dec. 2016.